Carrier conduction mechanism for phosphorescent material doped organic semiconductor

Seunguk Noh, C. K. Suman,[a] Yongtaek Hong, and Changhee Lee[b]
School of Electrical Engineering and Computer Science, Inter-University Semiconductor Research Center, Seoul National University, Seoul 151-744, Republic of Korea

(Received 6 November 2008; accepted 11 December 2008; published online 5 February 2009)

The mobility of charge carriers has been investigated in the pristine and phosphorescent material doped 4,4′,4″-tris(*N*-carbazolyl) triphenylamine (TCTA) using time-of-flight photoconductivity technique. Doping phosphorescent material fac-tris(2-phenylpyridine) iridium [$Ir(ppy)_3$] increases the electron mobility whereas the hole mobility decreases to the order of 10^{-4}–10^{-6} $cm^2/V\,s$ measured at room temperature with different bias voltages. The analysis of field and temperature dependences of the mobility agrees well with the Gaussian disorder model. The calculated positional disorders (Σ) for TCTA, $Ir(ppy)_3$-doped TCTA, and tris(1-phenylisoquinoline) iridium [$Ir(piq)_3$] -doped TCTA are 0.12, 2.05, and 1.62 for hole, respectively; 3.89 for electron in only $Ir(ppy)_3$-doped TCTA. The ambipolar transport for holes and electrons is possible by doping TCTA with $Ir(ppy)_3$ (green dopant) whereas only hole transport with reduced mobility is achieved for $Ir(piq)_3$ (red dopant). © *2009 American Institute of Physics*. [DOI: 10.1063/1.3072693]

I. INTRODUCTION

There is an increasing interest of using organic semiconductors for device applications such as organic light emitting diodes (OLEDs),[1–4] organic solar cells,[5,6] and organic field effect transistors.[7,8] The device efficiency and functionality are controlled by engineering the carrier transport properties of organic semiconductors. The transport properties can be manipulated by morphological structure, doping, electric field, and temperature. The harvesting of both singlet and triplet excitons by doping phosphorescent materials in the organic semiconductor host can produce more than 20% external quantum efficiency in phosphorescent OLEDs.[9,10] The charge transport and the exciton formation zone are closely related to each other.[11,12] Hence, there is a need of deep understanding of carrier transport properties of phosphorescent material doped organic semiconductors.

The time-of-flight photoconductivity (TOF-PC) is a powerful method for charge transport analysis in bulk organic system.[13] In this method, the sample is photoexcited using a pulse laser and the transit time of the charge carriers across the film is measured in the photocurrent transients.[13,14] Generally, the film thickness should be a few micrometers so that the excitation light is absorbed in very thin layer compared to the total thickness of the film.[15] The field and temperature dependences of the mobility have been analyzed by a Gill-modified Poole–Frenkel (PF) equation,[16] Gaussian disorder model (GDM) suggested by Bässler,[17] and correlated disorder model[18,19] for organic semiconductor. The Gill analysis can predict the negative field dependence of the mobility as well as an exponential dependence on the square root of the electric field.[16] The disorder formalism describes the hopping transport of carriers in terms of the positional and energetic disorders of organic materials.[17] In this paper we report the temperature and electric field dependences of carrier mobilities measured in 4,4′,4″-tris(*N*-carbazolyl) triphenylamine (TCTA) and phosphorescent material [$Ir(ppy)_3$ and $Ir(piq)_3$] doped TCTA. The carrier transport is analyzed by Bässler's GDM.[17]

II. EXPERIMENT

The glass substrates precoated with indium-tin-oxide (ITO) were cleaned using isopropyl alcohol, de-ionized water, acetone, methanol in an ultrasonic bath for 10 min and dried into an oven at 120 °C more than 30 min. The ITO substrates were exposed to ultraviolet ozone treatment for 5 min prior to loading into vacuum chamber. TCTA, TCTA:$Ir(ppy)_3$, and TCTA:$Ir(piq)_3$ layers were deposited by thermal evaporation under $<5\times10^{-6}$ Torr without breaking vacuum. The deposition rate of organic layers was controlled at 0.1–0.3 nm/s and the doping ratio was controlled about 7% by monitoring a quartz crystal oscillator. The thicknesses of TCTA, TCTA:$Ir(ppy)_3$, and TCTA:$Ir(piq)_3$ films were 1.31, 1.16, and 1.3 μm, respectively. Semitransparent Al electrodes were deposited on the organic films with the overlap area of the Al and ITO electrodes about 2 mm^2. The samples were loaded on to the cold finger of the closed-cycle cryostat and the TOF-PC mobility was measured from 200 to 320 K. In the TOF-PC measurements, the devices were applied from 5 to 110 V by a dc power supply (Agilent E3612A) and illuminated through Al or ITO electrodes using a nitrogen pulse laser with the wavelength of 337 nm and the pulse duration of 600 ps (PTI GL 3300). The TOF transients were monitored with a digital oscilloscope (Tektronix TDS 5054B).

III. RESULTS AND DISCUSSION

Figure 1 shows the photocurrent transients at room temperature of TCTA, and $Ir(ppy)_3$- and $Ir(piq)_3$-doped TCTA in

[a]Electronic mail: cksuman@gmail.com.
[b]Electronic mail: chlee7@snu.ac.kr.

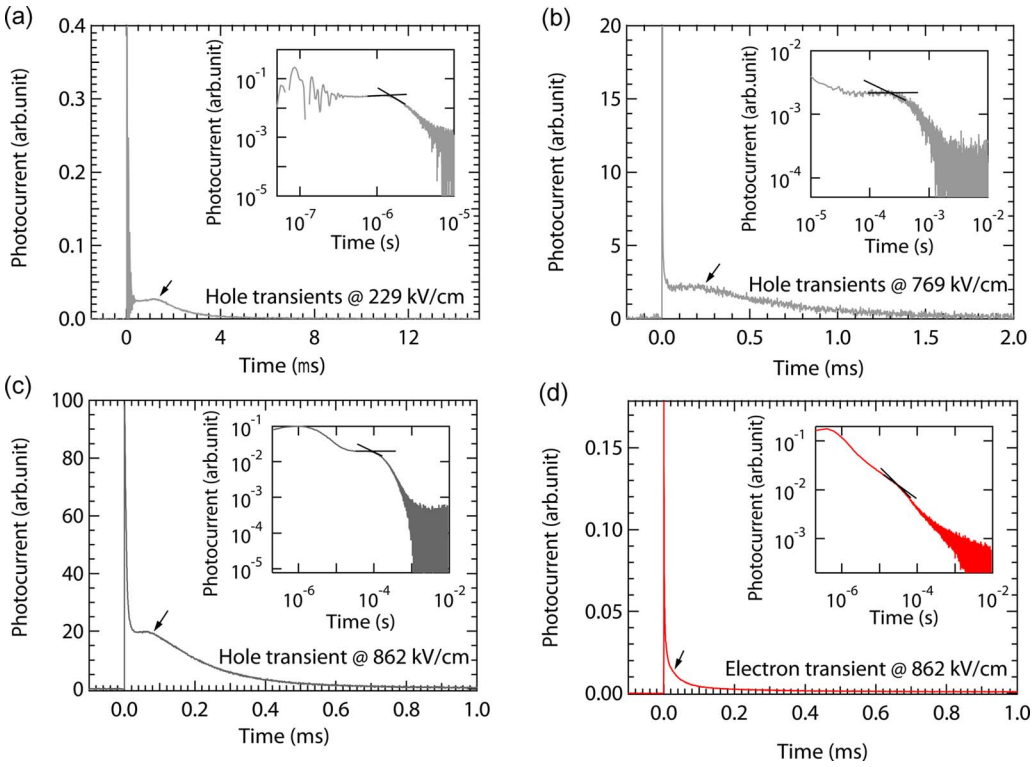

FIG. 1. (Color online) Photocurrent transients of (a) TCTA for hole, (b) $Ir(piq)_3$-doped TCTA for hole, (c) $Ir(ppy)_3$-doped TCTA for hole, and (d) for electron; at the room temperature in a linear scale; the inset plots the data in a log-log scale (the arrow in the figures indicates the transit time).

a linear scale and a log-log scale in the inset. The hole photocurrent plateaus in the pristine and phosphorescent material doped TCTA films indicate that hole transport is nondispersive. The intersection of asymptotes to the plateau and the tailing edge of the photocurrent transients gives the transit time (t_{tr}) of the carriers. The electron photocurrent transients in doped TCTA measured with a reversed polarity field show temporal decays, which correspond to dispersive transport of electrons. The transit time is related to the carrier mobility by the relation

$$\mu = \frac{d^2}{Vt_{tr}}, \tag{1}$$

where d is the film thickness and V is the applied voltage.

Figure 2 shows the field dependence of the hole mobility of pristine material doped TCTA at temperatures from 200 to 320 K. At the low field, the mobility is almost independent of the field for pristine TCTA at room temperature. At higher fields, the mobility increases exponentially with the square root of the field E, consistent with the PF relation

$$\mu = \mu_0 \exp(\beta\sqrt{E}), \tag{2}$$

where μ_0 is the zero-field mobility; the calculated values of zero field mobility and β (PF slope) have been analyzed by the GDM. In the disordered organic materials the conduction is considered as the hopping over an ensemble of transport sites. Each molecule is considered as a transport site for charge conduction. In hopping transport the charge conduction is thermally activated and is therefore temperature dependent. Similarly, the zero-field mobility and the PF slope (β) were calculated for $Ir(ppy)_3$- and $Ir(piq)_3$-doped TCTA from the field dependence of the mobility at different temperatures [Figs. 2(b)–2(d)]. The electron mobility could be measured only in the $Ir(ppy)_3$-doped TCTA and its field and temperature dependences are shown in Fig. 2(d).

Both electron and hole mobilities follow the PF relation with the field. The doping of organic materials gives rise to mainly energy traps, changes in energy width (σ) of the hopping sites, and the positional or orientational (Σ) disorder due to distribution of intersite distances. The carrier mobility dependence on these disorders can be represented by a semiempirical equation (GDM).[17]

$$\mu(E,T) = \mu_{inf} \exp\left[-\left(\frac{2\sigma}{3k_BT}\right)^2\right]\exp(\beta\sqrt{E}) \tag{3}$$

and

$$\beta = C\left[\left(\frac{\sigma}{k_BT}\right)^2 - \Sigma^2\right], \tag{4}$$

where T is the absolute temperature, k_B is the Boltzmann constant, μ_{inf} is the high temperature limit of the mobility, and C is a constant.

Figure 3 shows the variation of zero-field hole mobility with inverse of temperature square ($1/T^2$) for both doped and undoped TCTA; the inset shows the zero-field electron mobility in $Ir(ppy)_3$-doped TCTA. The linear fitting for zero-field hole mobility from temperature 200 to 320 K for pristine TCTA is a straight line, corresponding to no transition of dispersive to nondispersive (D-ND) in this temperature range. The onset of the D-ND transition occurs below 100 K (calculated value of 94.53 K). This transition temperature has been calculated using the proposed Bässler model equation

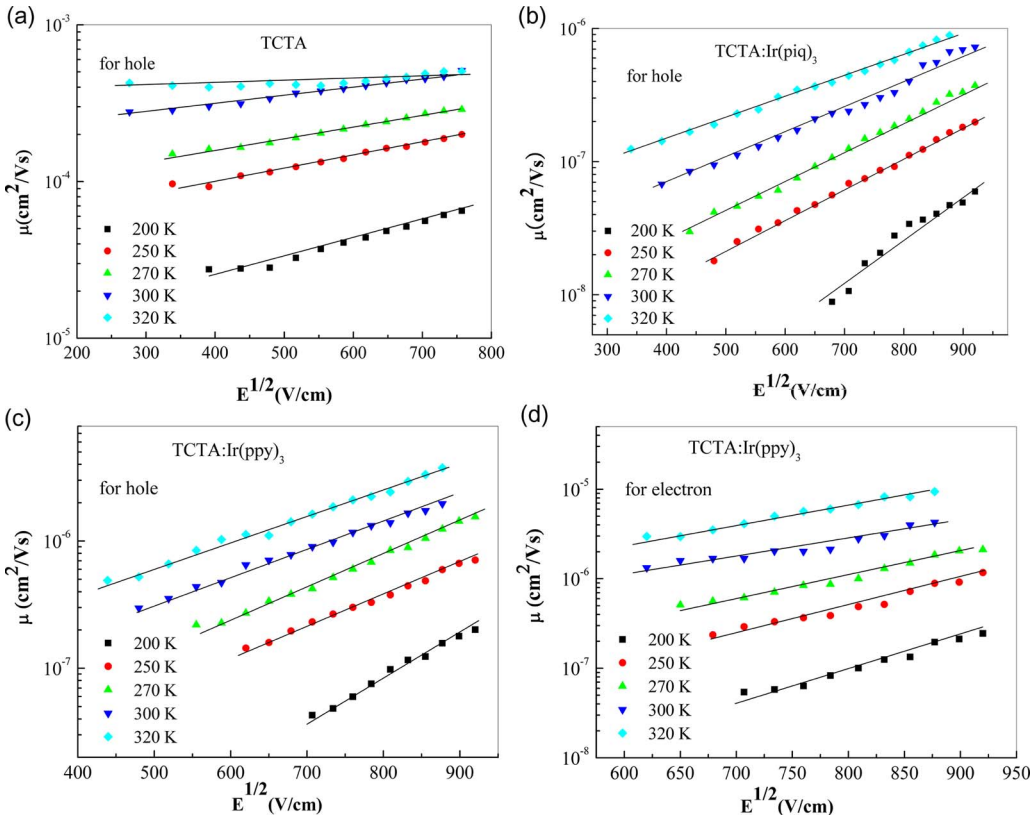

FIG. 2. (Color online) The field dependence of hole mobility in (a) TCTA, (b) $Ir(piq)_3$-doped TCTA, (c) $Ir(ppy)_3$-doped TCTA, and (d) electron mobility for $Ir(ppy)_3$-doped TCTA at different temperatures.

$$\left(\frac{\sigma}{k_B T_C}\right)^2 = 44.8 + 6.7 \log d, \tag{5}$$

where d is the thickness of the sample in centimeters.

Figure 4 shows the onset of the D-ND transition temperature for $Ir(piq)_3$-doped TCTA at 230 K; the inset shows the photocurrent transients at 200 K, dispersive signal, and 250 K, nondispersive signal. The transition temperature of $Ir(ppy)_3$-doped TCTA is around 225 K (calculated value). Although the transition temperature for pristine TCTA and $Ir(ppy)_3$-doped TCTA is not clearly observed experimentally but the transition temperature for $Ir(piq)_3$-doped TCTA calculated by Bässler's model[17] agrees well with the experimental value. The linear fit field independent mobility gives the values of the width of Gaussian density of states (σ), which have been shown in Table I. There is a very minor change in the Gaussian density of states for holes in doped and undoped TCTA whereas the hole mobility decreases by two orders of magnitude. The energy traps or the dispersion of carriers may be responsible for this decrease.[18,20] The dopant

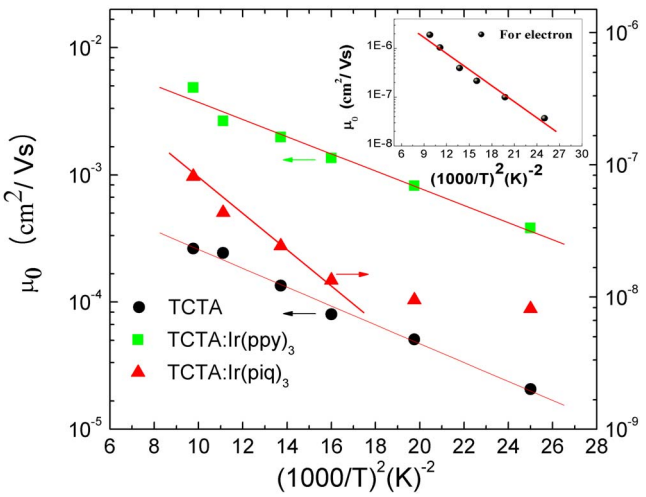

FIG. 3. (Color online) The zero-field mobility μ_0 vs $1/T^2$ of hole mobility in TCTA, and $Ir(ppy)_3$- and $Ir(piq)_3$-doped TCTA; the inset is the μ_0 for electron in the $Ir(ppy)_3$-doped TCTA.

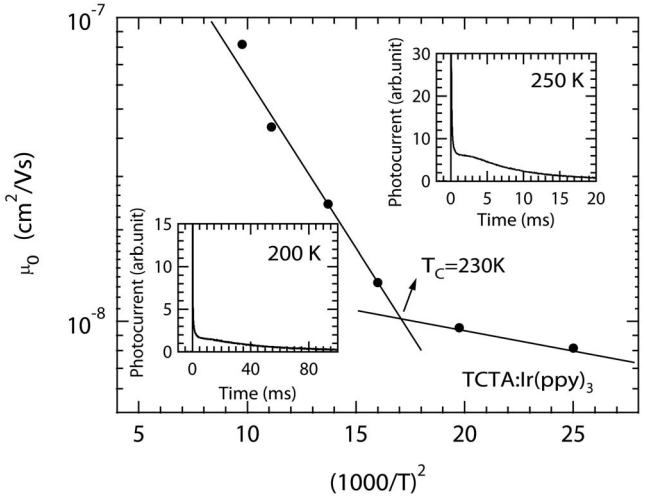

FIG. 4. The zero-field mobility μ_0 vs $1/T^2$ of hole mobility in $Ir(piq)_3$-doped TCTA; the inset is the hole photocurrent transients at 200 and 250 K.

TABLE I. Carrier transport parameters of pristine material doped TCTA.

	W	σ (meV)	Σ	C $(\mathrm{cm/V})^{1/2}$
TCTA	0.41	35.28	0.12	2.90×10^{-4}
TCTA:Ir(ppy)$_3$	0.62	32.94	2.05	5.72×10^{-4}
	0.53	43.14(forelectron)	3.89	3.34×10^{-4}
TCTA:Ir(piq)$_3$	0.62	44.84	1.62	3.41×10^{-4}
Errors (%)	~10	~2	~10	<5

induced traps capture holes during their transit. The charge carriers are thermally released from the traps where these are immobilized.

In local thermal equilibrium, the effective mobility (μ_{eff}) in a system with traps and the mobility (μ_0) of the undoped system are related to the equation[19]

$$\frac{\mu_{\mathrm{eff}}}{\mu_0} = [1 + c\,\exp(\Delta E/k_B T)]^{-1}, \tag{6}$$

where c is the trap concentration, ΔE is the trap depth, and T is the temperature. The value of trap depth is calculated as 12.02 meV, which is within the energy difference of TCTA and Ir(ppy)$_3$. However, this value is very low; this difference may be due to the assumption of the monoenergetic trap level in the above model. The energetic distribution of trap states also plays a role in lowering the hole mobility.

Figure 5 shows the variation of field dependent PF slope β with inverse of temperature square $(\sigma/k_B T)^2$ for hole transport in TCTA and doped TCTA; the inset shows the same for electron in doped TCTA. The values of positional or orientational disorder (Σ) and the constant (C) have been calculated by fitting the data using Eq. (4). Table I shows that the positional disorder increases with doping of TCTA. Besides the effect of doping on disorder, the carrier dispersion is also affected by the doping. The degree of carrier dispersion in organic materials can be calculated by the tail broadening parameter W,[21]

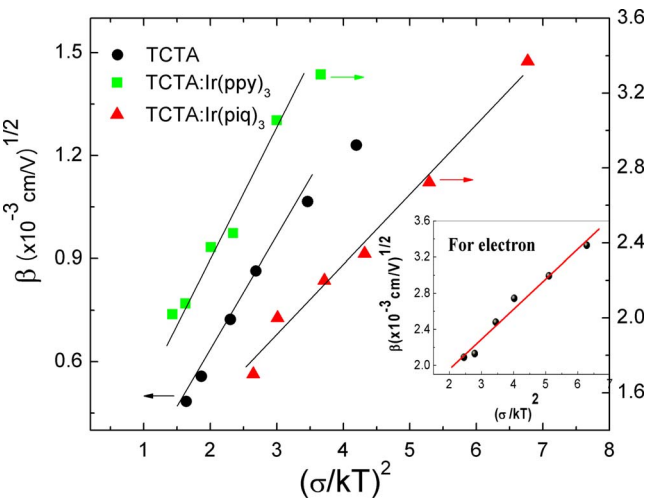

FIG. 5. (Color online) The field dependence of PF slope β vs $1/T^2$ for hole in TCTA and doped TCTA; the inset shows the same for electron in the Ir(ppy)$_3$-doped sample.

$$W = \frac{t_{1/2} - t_{\mathrm{tr}}}{t_{1/2}}, \tag{7}$$

where t_{tr} is the transit time of the leading carriers and $t_{1/2}$ is the time after which the current has decreased to half of its plateau value. The extracted values of W are summarized in Table I. The large value of W can be associated with a high degree of dispersion after doping TCTA. It is also worthwhile to note that electron and hole mobilities in the Ir(ppy)$_3$-doped TCTA are of the same order. Therefore, the ambipolar transport of holes and electrons can be possible in the Ir(ppy)$_3$-doped TCTA. This result suggests that one can use the Ir(ppy)$_3$-doped TCTA as an ambipolar host layer for the red phosphorescent emitters. The balance of electron and hole transport can be achieved by doping appropriate concentrations of Ir(ppy)$_3$ in TCTA, leading to high electroluminescence efficiency.[22]

IV. CONCLUSIONS

The influence of charge trapping, scattering, and disorder on charge transport has been studied in pristine TCTA and TCTA doped with phosphorescent dopants. The hole transport in undoped and doped TCTA is nondispersive whereas the electron transport in doped TCTA is dispersive. The hole mobility decreases by two orders of magnitude due to additional trap residing times. However, the electron gets favorable hopping sites for conduction in Ir(ppy)$_3$-doped TCTA. The tail broadening parameter reveals by doping and charges travel longer transit path due to carrier scattering. The positional or orientational disorders for TCTA, and Ir(ppy)$_3$- and Ir(piq)$_3$-doped TCTA are 0.12, 2.05, and 1.62, respectively. The significant difference in all types of disorders (positional or orientational, and energetic) and the carrier dispersion are responsible for lowering of the hole mobility.

ACKNOWLEDGMENTS

This work was supported by Samsung SDI–Seoul National University Display Innovation Program (SSDIP).

[1] C. W. Tang and S. A. Vanslyke, Appl. Phys. Lett. **51**, 913 (1987).
[2] J. H. Burroughes, D. D. C. Bradley, A. R. Brown, R. N. Marks, K. Mackay, R. H. Friend, P. L. Burn, and A. B. Holmes, Nature (London) **347**, 539 (1990).
[3] M. A. Baldo, D. F. O'Brien, Y. You, A. Shoustikov, S. Sibley, M. E. Thompson, and S. R. Forrest, Nature (London) **395**, 151 (1998).
[4] J. P. J. Markham, T. D. Anthopoulos, I. D. W. Samuel, G. J. Richards, P. L. Burn, C. Im, and H. Bässler, Appl. Phys. Lett. **81**, 3266 (2002).
[5] C. W. Tang, Appl. Phys. Lett. **48**, 183 (1986).
[6] G. Yu, J. Gao, J. C. Hummelen, F. Wudl, and A. J. Heeger, Science **270**, 1789 (1995).
[7] H. Sirringhaus, N. Tessler, and R. H. Friend, Science **280**, 1741 (1998).
[8] F. Garnier, R. Hajlaoui, A. Yassar, and P. Srivastava, Science **265**, 1684 (1994).
[9] Y. Sun, N. C. Giebink, H. Kanno, B. Ma, M. E. Thompson, and S. R. Forrest, Nature (London) **440**, 908 (2006).
[10] G. He, M. Pfeiffer, K. Leo, M. Hofmann, J. Brinstock, R. Pudzic, and J. Salbeck, Appl. Phys. Lett. **85**, 3911 (2004).
[11] B. D. Chin and C. H. Lee, Adv. Mater. (Weinheim, Ger.) **19**, 2061 (2007).
[12] H.-I. Baek and C. H. Lee, J. Appl. Phys. **103**, 054510 (2008).
[13] P. M. Borsenberger and D. S. Weiss, *Organic Photoreceptors for Imaging Systems* (Dekker, New York, 1993).
[14] R. G. Kepler, Phys. Rev. **119**, 1226 (1960).
[15] M. Redecker, D. D. C. Bradley, M. Inbasekaran, and E. P. Woo, Appl.

Phys. Lett. **73**, 1565 (1998).
[16]W. D. Gill, J. Appl. Phys. **43**, 5033 (1972).
[17]H. Bassler, Phys. Status Solidi **175**, 15 (1993) (b).
[18]S. V. Novikov, D. H. Dunlap, V. M. Kenkre, P. E. Parris, and A. V. Vannikov, Phys. Rev. Lett. **81**, 4472 (1998).
[19]K. K. Tsung and S. K. So, Appl. Phys. Lett. **92**, 103315 (2008).
[20]H. H. Fong and S. K. So, J. Appl. Phys. **100**, 094502 (2006).
[21]H. Tseng, T. Jen, K. Y. Peng, and S. Chen, Appl. Phys. Lett. **84**, 1456 (2004).
[22]S. U. Noh, C. K. Suman, and C. H. Lee (unpublished).